# Longitudinal Josephson-plasma excitation in $Bi_2Sr_2CaCu_2O_{8+\delta}$: Direct observation of the Nambu-Goldstone mode in a superconductor

K. Kadowaki

*Institute of Materials Science, The University of Tsukuba, Tsukuba, Ibaraki 305, Japan*

I. Kakeya

*Research Center for Materials Science at Extreme Conditions, Osaka University, Toyonaka, Osaka 560, Japan*

M. B. Gaifullin

*Department of Physics, Hokkaido University, Sapporo 060, Japan*

T. Mochiku

*National Research Institute for Metals, 1-2-1, Sengen, Tsukuba, Ibaraki 305, Japan*

S. Takahashi and T. Koyama

*Institute for Materials Research, Tohoku University, Katahira, Aoba-ku, Sendai 980, Japan*

M. Tachiki

*National Research Institute for Metals, 1-2-1, Sengen, Tsukuba, Ibaraki 305, Japan*

Electromagnetic resonant absorption phenomena in a microwave frequency range have recently been studied in the single-crystalline high-temperature superconductor $Bi_2Sr_2CaCu_2O_{8+\delta}$ in magnetic fields. Using a rectangular microwave cavity resonator technique with $TE_{102}$ mode this absorption is unambiguously identified to be the collective longitudinal Josephson plasma excitation. Since the superconducting state is a state with a broken phase symmetry, the ordered state should be accompanied by the collective excitation (Nambu-Goldstone mode). This excitation has long been thought not to be observable, because of the formation of the large Coulomb gap (Anderson-Higgs-Kibble mechanism), above which strong damping mechanisms of excited plasma are presumably present. However, this Coulomb gap can be very small in the case of anisotropic layered system such as $Bi_2Sr_2CaCu_2O_{8+\delta}$, and the plasma mode may lie in a microwave frequency region. Using characteristic dispersion relations, which enables us to separate out the longitudinal mode from the transverse one, the microwave absorption observed in $Bi_2Sr_2CaCu_2O_{8+\delta}$ is unambiguously attributed to the longitudinal excitations. We believe that this is the first and the direct experimental evidence of the Nambu-Goldstone mode in a superconductor and provides a direct proof that the Anderson-Higgs-Kibble (AHK) mechanism within the concept of spontaneously breaking symmetry is indeed valid in the case of superconducting phase transition. Since the finite plasma frequency observed here signifies formation of the finite mass of the plasma (phason) due to the AHK mechanism in the relativistic sense, the above-mentioned scenario in a superconductor corresponds to a direct mapping from the unified gauge-field theory of weak interaction and electromagnetic interaction shown by Weinberg and Salam. [S0163-1829(97)03734-X]

Soon after the BCS (Bardeen, Cooper, Schrieffer) theory of superconductivity,[1] a serious question in regard to their pairing theory was raised, i.e., violation of the gauge invariance. Even though the whole interaction Hamiltonian is taken into account, a new set of states of nonzero momentum must be present in the superconducting energy gap, which may lead to large perturbations in the ground state and may alter the low-temperature superconducting properties greatly. In order to overcome this problem, Anderson[2,3] has proposed an idea in which the long-range Coulomb interaction should be included in the BCS theory. By doing so, the low-lying excitations (Nambu-Goldstone mode[4,5]) associated with the superconducting phase transition is pushed away well above the superconducting energy gap by the formation of the Coulomb gap [Anderson-Higgs-Kibble (AHK) mechanism[2,3,6,7]] of $\sim$eV. Since such an electronic state cannot be distin-

guished from the normal state, it has been believed that the Nambu-Goldstone mode are unobservable until just recently.

According to the London electrodynamics in a highly layered superconductor such as $Bi_2Sr_2CaCu_2O_{8+\delta}$ [$\lambda_c/\lambda_{ab} = (m_c/m_{ab})^{1/2} \approx 300-1000$], the plasma frequency with the polarization for the perpendicular direction to the layers, $\omega_p^c = c/(\lambda_c \epsilon_\infty^{1/2})$, becomes very low, of the order of 1 meV, which lies much below the superconducting energy gap $\Delta(0) \approx 30$ meV in this compound,[8-10] whereas the plasma frequency in this case is $\omega_p^{ab} \approx 1$ eV. In such a condition, the plasma oscillation is predicted to be observable by experiments using electromagnetic excitations, since the damping mechanism is forbidden to occur. At a far-infrared frequency region around 20–50 cm$^{-1}$ Tamasaku, Nakamura, and Uchida[11] have pointed out the existence of a sharp plasma edge in the $c$-axis reflectivity measurements ($\mathbf{E} \| c$) in single-

crystal $La_{2-x}Sr_xCuO_4$. More recently, a sharp anomaly of the microwave surface resistance with an anticyclotronic behavior in a perpendicular field ($\mathbf{B}_{ext} \| c$) was discovered by Tsui *et al.*[12] and similarly a sharp microwave absorption by Matsuda *et al.*[13] and Kadowaki *et al.*,[14] both in single-crystalline $Bi_2Sr_2CaCu_2O_{8+\delta}$. In the latter experiment, in particular, the absorption is attributed to the Josephson plasma resonance.

The purpose of this paper is to report the experimental observation of the Nambu-Goldstone mode in a highly layered superconductor $Bi_2Sr_2CaCu_2O_{8+\delta}$ in a microwave frequency region (34–90 GHz) using a cavity resonator. Although similar experimental studies[12,13,15] have recently been reported, all these results have been treated as the transverse Josephson plasma[16,17] by the analogy with the Josephson plasma in a single Josephson junction,[18,19] in which the longitudinal plasma mode does not exist. Therefore, such a treatment for the present case is utterly insufficient and is even misleading to the wrong understanding of the collective excitations in the superconducting state. We have performed a careful examination of the experimental conditions and have compared the experimental results with the theory of Josephson plasma recently developed by Tachiki and his collaborators,[8,20,21] in which the longitudinal collective excitation is correctly treated. By doing so, it is found that, first the dispersion relations for the two plasma modes are very different, which enables us to distinguish them experimentally as described below. Second, the line shape predicted by the theory gives a distinct difference between longitudinal and transverse modes.

We begin by showing the experimental setting used in the experiments at 45 GHz in Fig. 1 in detail, since the geometrical arrangement between the sample and the microwave $\mathbf{E}_{rf}$ vector is crucially important for the longitudinal plasma excitation. To assign the plasma mode properly, it is best to use a rectangular cavity resonator with the fundamental mode in which the microwave $\mathbf{E}_{rf}$ and $\mathbf{H}_{rf}$ vectors have the separate standing modes. The sample, which is a piece of single-crystalline $Bi_2Sr_2CaCu_2O_{8+\delta}$ with a rectangular shape of 0.5 mm×0.5 mm×~20 $\mu$m cut from a larger piece, is mounted on the thin diamond bar sample holder (0.5 mm×0.35 mm×15 mm) by either Apiezon grease or GE varnish. The diamond bar holder is placed at the quarter position in a rectangular cavity resonator with $TE_{102}$ mode, where the microwave electric vector $\mathbf{E}_{rf}$ has a maximum intensity and the microwave magnetic vector $\mathbf{H}_{rf}$ has a node. The sample size is small enough compared with the cavity dimension of 4.775 mm×2.388 mm×9.3 mm. This ensures that the microwave $\mathbf{E}_{rf}$ vector is uniform and is exerted perpendicular to the *ab* plane of the sample. The incident microwave is modulated by pin diode electronically with a frequency of several Hz and the absorption signal from the bolometer located at the end of the sample holder is detected by lock-in technique. In order to obtain the absolute absorption power an identical diamond sample holder coated with Au is inserted at the another quarter position of the cavity as shown in Fig. 1.

A typical example of the resonance is shown in Fig. 2, where the power absorbed is shown as a function of $\mathbf{B}$ ($\mathbf{B}_{ext} \| c$) for three different temperatures. A characteristic feature here is that the resonance line has a symmetric shape
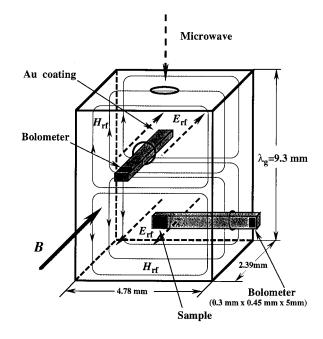


FIG. 1. A schematic drawing of the rectangular cavity resonator with $TE_{102}$ mode used for the experiments of longitudinal plasma. The dimensions are not in scale. The diamond sample holder on which a piece of single crystalline $Bi_2Sr_2CaCu_2O_{8+\delta}$ is glued is used as a bolometric detector, and is placed at the quarter position of the cavity where the microwave $E_{rf}$ vector is maximum. Another identical diamond sample holder with evaporated Au thin film is placed at the other quarter position of the cavity for the purpose of absorbed power calibration.

with a slight tail at the higher field side. Nevertheless, the level of the absorption spectrum eventually becomes nearly equal below and above the resonance position. The line shape does not show significant temperature dependence. It is noted that the resonance position, on the contrary, varies with temperature in a peculiar fashion, reflecting the dynami-
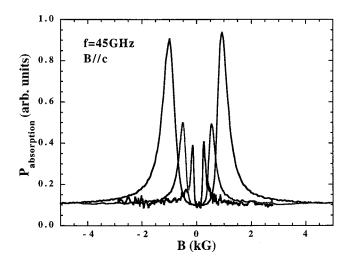


FIG. 2. A typical example of the microwave absorption spectrum at 45 GHz in a cavity shown in Fig. 1 in a perpendicular magnetic field ($\mathbf{B} \| c$) at three different temperatures. The resonances observes are plotted at 22.5 K (outer curve), 44.9 K (middle curve), and 66.9 K (inner curve). The vertical scale is taken arbitrarily but the relative intensity is kept unchanged.

cal nature of the vortex state in $Bi_2Sr_2CaCu_2O_{8+\delta}$ strongly.[13,14]

For the purpose of the discussion below, we have carefully checked our experimental conditions. The calibration of the absorbed power was done at each temperature to compare the relative intensity as a function of temperature. The microwave power dependence of the absorption intensity was also carefully checked and the linear response is confirmed in the present experiments. Furthermore, we checked the absence of the absorption in a configuration where the sample is placed at the half position of the $TE_{102}$ cavity mode, where the magnetic-field vector has a maximum and the electric vector has a minimum. In this configuration, two cases $H_{rf} \| ab$ and $H_{rf} \| c$ are examined. However, we failed to observe the resonance line in both cases, when the sample width is smaller than the critical size of $L_c \sim 1.2$ mm. From these experiments it is clearly excluded that the resonance absorption originates from either conventional magnetic or cyclotron resonances. We confirm from the angular dependence measurements that the perpendicular component of the electric field ($E_{rf} \| c$) is essential for the longitudinal plasma excitations.

In the following we will show theoretically how the resonance peak in the microwave absorption originates from the excitation of the longitudinal Josephson plasma in $Bi_2Sr_2CaCu_2O_{8+\delta}$. Let us consider a system whose dimension in the $c$ direction is $d$ and extended infinitely in the $ab$ plane. An oscillating electric field $E_0 \exp(-i\omega t)$ is applied uniformly in the $c$ direction. The electric field induces the interlayer Josephson current along the $c$ axis. In a magnetic field $B$ ($B_{ext} \| c$) the interlayer Josephson current, which is responsible for the occurrence of the Josephson-plasma oscillation, is strongly affected by the presence of vortices. The suppression of the interlayer Josephson current caused by the destruction of the interlayer phase coherence gives rise to the increase of the $c$-axis penetration depth $\lambda_c$ and, thus, the decrease of the Josephson plasma frequency $\omega_p = c/(\lambda_c \epsilon_\infty^{1/2})$, where $\epsilon_\infty$ is the high-frequency dielectric constant. In the following we include this effect phenomenologically in the $c$-axis penetration depth $\lambda_c(B)$. Thus, we express the current along the $c$ axis as

$$j_z = -\frac{c}{4\pi\lambda_c^2(B)} A_z + \sigma_{qp}(\omega,B) E_z, \qquad (1)$$

where $A_z$ is the $z$ component of the vector potential. The first and second terms in Eq. (1) are the superconducting and the quasiparticle currents, respectively. $\sigma_{qp}(\omega,\mathbf{B})$ is the quasiparticle conductivity, $\lambda_c$ is related to the effective interlayer Josephson critical current $j_c(\mathbf{B})$ as $\lambda_c(B) = [c\Phi_0/8\pi^2 j_c(B)s]^{1/2}$, where $\Phi_0$ is the flux quantum, and $s$ is the interlayer spacing. Equation (1) is valid in the case of slow variation of $A_z$ along the $c$ axis, i.e., the wavelength of the plasma is much larger than the spacing $s$. The charge is induced in response to the scalar potential $A_0$ as

$$\rho = -\frac{1}{4\pi\mu^2} A_0, \qquad (2)$$

where $\mu$ is an effective charge screening length along the $c$ axis due to the superconducting carriers and quasiparticles.
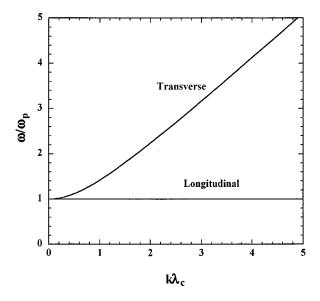


FIG. 3. The dispersion relations of Josephson plasma for transverse and longitudinal modes. The flat dispersion of the longitudinal plasma mode is due to the extremely small value of $\epsilon_\infty \mu^2 k_{2n+1} \approx 6.2 \times 10^{-7} \ll 1$ for $\epsilon_\infty \approx 25$, $\mu \approx 10$ Å and $k_{2n+1} = \pi/L \approx 1.57 \times 10^3$ with $L = 20$ $\mu$m and $n = 0$, compared with the value of $\lambda_c k_{2n+1} \approx 1$ for the transverse plasma mode.

In the oxide superconductors $\mu$ is the order of the interlayer distance. The $A_z$ and $A_0$ are related to the electric field $E_z$ as $E_z = -(1/c)\partial A_z/\partial t - \partial A_0/\partial z$. Combining Eqs. (1) and (2) with the Maxwell's equations and the boundary condition for the electric field, we obtain the longitudinal electric field $E_z(z,\omega)$ which consists of a series of standing waves inside the sample:

$$E_z = \frac{4E_0}{L} e^{-i\omega t} \sum_{0<k_n} \frac{\sin(k_{2n+1}z)}{k_{2n+1}\epsilon_L(k_{2n+1},\omega)}, \qquad (3)$$

where $\epsilon_L(k_{2n+1},\omega)$ is the longitudinal dielectric function given by

$$\epsilon_L(k_{2n+1},\omega) = \epsilon_\infty + \frac{\epsilon_\infty - 4\pi i \omega \sigma_{qp}(\omega,B)/\omega_p^2(B)}{\omega_\infty \mu^2 k_{2n+1}^2 - \omega^2/\omega_p^2}, \qquad (4)$$

where $\omega_p(B) = c/\{\lambda_c(B)\epsilon_\infty^{1/2}\}$, $\epsilon_\infty$ being the high-frequency dielectric constant and $k_{2n+1} = \pi(2n+1)L$ with $n$ being integers. The electric field of Eq. (3) has resonance peaks at longitudinal plasma frequencies of $\omega_L(k_{2n+1}) = \omega_p(B)[1 + \epsilon_\infty \mu^2 k_{2n+1}^2]^{1/2}$, which yields the dispersion relation as shown in Fig. 3. It is noted that the longitudinal mode has a characteristic flat dispersion relation, whereas the transverse one $\omega_T(k_{2n+1}) = \omega_p(B)[1 + \lambda_c^2 k_{2n+1}^2]^{1/2}$, which can be obtained in a similar manner,[8] shows a strong dispersion, and eventually tends to the linear dependence for $k \to \infty$. This difference in the dispersion relation is used to distinguish two plasma modes as discussed below.

The transverse mode can be excited in accordance with the dispersion relation with discrete energies depending on $k_{2n+1} = \pi(2n+1)/L$, since $\lambda_c$ is very large, $\sim 10^{-2}$ cm, and the sample size, $L \sim 1-3$ mm, is comparable with the wavelength inside the sample. This means that the resonance line
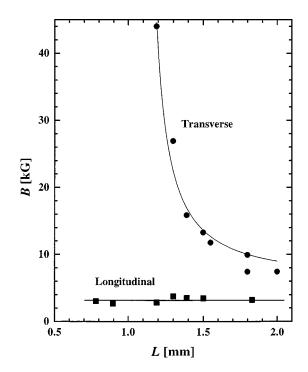
FIG. 4. The size dependence of the longitudinal and transverse plasma modes at 35 GHz. The divergent behavior of the resonance position is a characteristic behavior of the transverse plasma mode (filled circles) as the sample size is reduced close to the critical size $L_c = \pi c / \omega \epsilon_\infty^{1/2} \sim 1.2$ mm, whereas it is independent of $L$ for the longitudinal plasma mode (squares). The solid curve is the fitted curve to the formula $B_n = B_0 / \{1 - [(2n+1)\pi(c/\epsilon_\infty^{1/2}\omega L)]^2\}$ predicted by the transverse plasma mode. $\epsilon_\infty \approx 15$ is obtained as a fitting parameter.

should have a distinct sample size dependence, and multi-resonance lines may be expected with respect to the different $k$ values. According to the more elaborate theoretical analysis of the transverse plasma mode[22] one shows that the resonance field $B_n$ at a constant $\omega$ obeys a relation of $B_n = B_0 / \{1 - [(2n+1)\pi(c/\epsilon_\infty^{1/2}\omega L)]^2\}$, where $B_0$ is the resonance field with sufficiently large $L$ and $n$ is the number of the resonance lines corresponding to the different $k_{2n+1}$ values.

Based on this analysis, the size effect of the transverse plasma mode has been measured, which can be excited by the configuration with $\mathbf{H}_{rf} \| ab$ with the condition of $L > L_c = \pi c / \epsilon_\infty^{1/2} \omega$. The result is shown in Fig. 4, where the characteristic diverging behavior of $B_n$ is evident as $L \sim L_c$, in excellent agreement between theoretical prediction (solid line) and experiment (filled circles). It is stressed here that disappearance of the resonance line in samples smaller than $L_c$ is the characteristic feature of the transverse mode and does not exist in the longitudinal one. This experimental fact unambiguously confirms the separation of the longitudinal plasma mode from the transverse one even at $k \sim 0$, where both modes are nearly degenerated.

In the microwave experiment the power absorption is usually measured by varying the external magnetic field $\mathbf{B}$ at a fixed frequency of the microwave $\omega = \omega_0$. The power absorption $\rho = \mathrm{Re} j \cdot \mathrm{Re} E$ for the longitudinal plasma excitation by joule heating in the sample is given by
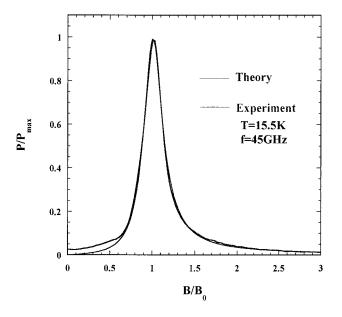


FIG. 5. The direct comparison of the absorption curve obtained from the experiments (thicker curve) with the calculated microwave power absorption spectrum (thinner curve) at 45 GHz as a function of $B$ applied along the $c$ axis using Eq. (5). The values of $\mu = 15$ Å and $L = 20$ $\mu$m are used for numerical calculations.

$$\rho = \frac{1}{2} \mathrm{Re}\{\sigma_{qp}(\omega)\} \langle |E_z(z,\omega)|^2 \rangle$$

$$= \mathrm{Re}\{\sigma_{qp}(\omega)\} E_0^2 \sum_{0 < k_n} \frac{4}{L^2 k_{2n+1}^2 |\varepsilon_L(k_{2n+1},\omega)|^2}, \quad (5)$$

where $\langle \rangle$ denotes the spatial average over the sample. The experimental results indicate that the plasma frequency $\omega_p(B)$ depends on the external field $\mathbf{B}$ as $\omega_p(B) = \beta B^{-1/2}$, which enables us to rewrite $\omega/\omega_p(B)$ as $(B/B_0)^{1/2}$, where $B_0 = \beta^2/\omega^2$ is the resonance field. Using these relations in Eqs. (3) and (4), we obtain $\rho$ as a function of $B/B_0$ as shown in Fig. 5. In the calculation, we assumed the $d$-wave pairing state with $d_{x^2-y^2}$ symmetry for which $\sigma_{qp}(\omega) = \alpha\omega$. The parameter values are taken as $\epsilon_\infty = 25$, $L = 2 \times 10^5$ Å, $\mu = 15$ Å, and $\alpha = 0.2$. As seen in Fig. 5, the calculated resonance peak is slightly asymmetric with a slight tail at the higher field side, in excellent agreement with the experimental result. Such an asymmetric resonance peak originates from the extremely small dispersion relation, which corresponds to the longitudinal plasma mode and not to the transverse one as discussed above. From this argument as well as the clear experimental mode separation as shown in Fig. 4, it is unambiguously concluded that the sharp resonance peak in a sufficiently smaller sample observed in $Bi_2Sr_2CaCu_2O_{8+\delta}$ ($\mathbf{E}_{rf}\|c$) arises from the resonant excitation of the longitudinal Josephson plasma (Nambu-Goldstone mode) at $k \approx 0$. We believe that this is an observation of the Nambu-Goldstone mode associated with the broken phase symmetry in a superconductor.

The resonance frequency of the longitudinal plasma becomes $\omega_L \approx \omega_p$ for $k \approx 0$, so that it is directly proportional to the critical superconducting current $j_c^{1/2}$ along the $c$ axis, which originates from the interlayer superconducting phase coherence $\langle \cos\varphi \rangle$, where $\varphi$ is the gauge-invariant phase dif-

ference between $l$th and $l+1$th layer given by $\varphi = \varphi_{l+1} - \varphi_l - \int A_z(z,t)dz$. It is experimentally observed that the resonance absorption so far studied at the lowest frequency of 34 GHz always begins to show up just below the bulk $T_c$ from zero field. This is carefully examined for many samples with different $T_c$ with different doping levels. It is concluded from this fact that the bulk superconductivity observed at $T_c$ is realized by the occurrence of the $c$-axis coherent supercurrent, which is maintained with the phase coherence along the $c$ axis. A similar result has been obtained from the direct $I$-$V$ characteristic measurement along the $c$ axis[23] previously. These phenomena at least imply that the occurrence of the superconductivity at $T_c$ is driven by the formation of the finite coherent critical current $j_c$ along the $c$ axis. Although the formation of the gap in a single-particle excitation spectrum which strongly suggests the existence of preformed Cooper pairs, has recently been observed well above $T_c$,[24] it is perhaps a state without interlayer superconducting coherence along the $c$ axis.

The finite plasma frequency $\hbar\omega_p$ at $k \approx 0$ means the formation of the rest mass of the plasma $m_p = \hbar/c\lambda\,\epsilon_\infty^{1/2}$ defined by $E = m_p c^2 = \hbar\omega_p$, which results from the wave equation $\Box B_\mu = -\lambda_c^{-2} B_\mu$, where $\Box \equiv \partial^\mu \partial_\mu = \partial^2/c^2\partial t^2 - (\partial^2/\partial x^2 + \partial^2/\partial y^2 + \partial^2/\partial z^2)$. Within the framework of the spontaneous symmetry-breaking concept in the superconducting phase transition the longitudinal plasma (Nambu-Goldstone mode) has long been a conjecture, which strongly relies on the AHK mechanism since the lack of experimental proof in the past. Here, our observation of plasma gap with the finite frequency $\omega_p$ at $k \approx 0$ is a direct experimental proof of the existence of the mass $m_p$ of the Nambu-Goldstone mode, which, at the same time, signifies validity of the AHK mechanism. Such a scenario is analogous to the current unified field theory in the elementary particle physics, and superconductivity is an extremely useful example, as good as high-energy experiments, to test the field theory.

Since the Josephson plasma resonance is a new phenomenon in the field of superconductivity and has a variety of unusual properties as functions of frequency $\omega$, applied magnetic field $\mathbf{B}$ and its relative orientation with respect to the crystal, anisotropy $\gamma$, the state of pinning, etc., most of which have not been studied so far in detail, it provides us a unique opportunity to study new aspects of superconductivity, in particular, in high-temperature superconductors, from the point of view of both fundamental physics and various applications.

[1] J. Bardeen, L. N. Cooper, and J. R. Schrieffer, Phys. Rev. **108**, 1175 (1957).

[2] P. W. Anderson, Phys. Rev. **110**, 827 (1958).

[3] P. W. Anderson, Phys. Rev. **112**, 1900 (1958).

[4] Y. Nambu, Phys. Rev. Lett. **4**, 380 (1960).

[5] Y. Nambu and G. Jona-Lasinio, Phys. Rev. **122**, 345 (1961).

[6] P. W. Higgs, Phys. Rev. Lett. **13**, 508 (1964).

[7] T. W. B. Kibble, Phys. Rev. **155**, 1554 (1967).

[8] M. Tachiki, T. Koyama, and S. Takahashi, Phys. Rev. B **50**, 7065 (1994).

[9] H. A. Fertig and S. Das Sarma, Phys. Rev. Lett. **65**, 1482 (1990).

[10] L. N. Bulaevskii, M. P. Maley, and M. Tachiki, Phys. Rev. Lett. **74**, 801 (1995).

[11] K. Tamasaku, Y. Nakamura, and S. Uchida, Phys. Rev. Lett. **69**, 1455 (1992).

[12] Ophelia K. C. Tsui, N. P. Ong, Y. Matsuda, Y. F. Yan, and J. B. Peterson, Phys. Rev. Lett. **73**, 724 (1994).

[13] Y. Matsuda, M. B. Gaifullin, K. Kumagai, K. Kadowaki, and T. Mochiku, Phys. Rev. Lett. **75**, 4512 (1995).

[14] K. Kadowaki, M. Gaifullin, Y. Matsuda, K. Kumagai, T. Mochiku, S. Takahashi, and M. Tachiki, in *Proceedings of the 8th International Workshop on Critical Currents in Superconductors*, edited by T. Matsushita and K. Yamafuji (World Scientific, Singpore, 1996), p. 235–238.

[15] Ophelia K. C. Tsui, N. P. Ong, and J. B. Peterson, Phys. Rev. Lett. **76**, 819 (1996).

[16] L. N. Bulaevskii, V. L. Pokrovsky, and M. P. Maley (unpublished).

[17] L. N. Bulaevskii, M. Maley, H. Safar, and D. Domínguez, Phys. Rev. B **53**, 6634 (1996).

[18] P. W. Anderson, in *Weak Superconductivity: The Josephson Tunneling Effect*, Lectures on the Many-body Problems, the 5th International School of Physics, Ravello, Italy, 1963, edited by E. R. Caianiello (Academic, New York, 1964), Vol. 2, p. 113.

[19] A. J. Dahm, A. Denenstein, T. F. Finnegan, D. N. Langenberg, and D. J. Scalapino, Phys. Rev. Lett. **20**, 859 (1968).

[20] M. Tachiki, T. Koyama, and S. Takahashi, Physica C **263**, 1 (1996).

[21] M. Tachiki, T. Koyama, and S. Takahashi, in *Coherence in High Temperature Superconductors*, edited by G. Deutscher and A. Revcolevschi (World Scientific, Singapore, 1996), p. 371.

[22] S. Takahashi, M. Tachiki, and K. Kadowaki (unpublished).

[23] K. Kadowaki and T. Mochiku, Physica B **194-196**, 2239 (1994); K. Kodowaki, T. Mochiku, H. Takeya, K. Hirata, and Y. Saito, Physica C **235-240**, 3275 (1994); T. Koyama and M. Tachiki (unpublished).

[24] H. Ding, T. Yokoya, J. C. Campuzano, T. Takahashi, M. Randeria, M. R. Norman, T. Mochiku, K. Kadowaki, and J. Giapintzakis, Nature (London) **382**, 51 (1996).